

EFFECTS OF MICRO-FIBRES ON EARLY-AGE PROPERTIES OF CONCRETE

Duy H. NGUYEN¹, Vinh T.N. DAO^{1,*}, Liza O'MOORE¹, Peter DUX¹

¹ School of Civil Engineering, the University of Queensland, Australia

*Email: v.dao@uq.edu.au

ABSTRACT

Proper control of early-age cracking risk in concrete as well as optimisation of relevant processes in precast industry requires an adequate knowledge of tensile and fracture properties of concrete at relevant ages. Despite significant past research, such knowledge is currently lacking. This paper presents the recent results of an ongoing research program aimed to address that important knowledge gap. After briefly outlining notable features of an improved direct tensile testing system, the paper presents key results of an experimental investigation into the tensile properties of concrete of age between 2.5 and 9 hours after mixing, both with and without fibres. Compared to concrete without micro-fibre, micro-fibre concrete is found to have more bleeding, considerably lower and more scattered tensile strength and Young's modulus, and higher fracture energy and characteristic length. Possible explanations for such differences are also given. Importantly, the roles of micro-fibres in mitigating the risk of plastic shrinkage cracking are shown to be complex, prompting the need for further study: Although a decreased tensile strength heightens such risk, an increased bleeding helps reduce the risk while the higher fracture energy and characteristic length implies higher ductility.

KEYWORDS

Early-age concrete, tensile properties, fracture properties, direct tensile test, micro fibre, digital imaging correlation.

INTRODUCTION

Knowledge of tensile properties of concrete from very early ages is essential for effective control of both early-age cracking and young concrete in precast industry:

- Early-age cracking may occur in concrete structures from as early as several hours after casting. The underlying mechanism for such cracking is the tensile stress due to restrained deformation reaching the concrete's tensile capacity at that age. Once occurred, existing cracks would develop further if sufficient energy is provided. Indeed, very often, cracks developed at early-ages would propagate and become unserviceable at later stages due to subsequent shrinkage/loading.

These cracks and their further development at later ages can seriously compromise the integrity, durability, aesthetics, and long-term service life of wide-ranging types of concrete structures. Highway pavements, bridge decks, industrial and residential floors, wharves, podiums, and parking structures, to name a few, are all susceptible to this type of cracking. The current trend of increasing use of concrete mixes with lower water-binder ratios, lower bleed capacities, and higher contents of cement and fine materials, increases the susceptibility of concrete structures to early-age cracking (Wiss, 2011). As a result, despite significant past research (R Springenschmid, 1994; R. Springenschmid, 1998; Wiss, 2011), early-age cracking remains widespread and indeed among the major causes of concrete structures' deterioration (Byard et al., 2010).

- In precast industry, it is highly desirable to release pre-tensioned forces, demoulding and freeing up the casting area as soon as possible, while restricting prestress loss as well as ensuring adequate concrete properties upon releasing (Hernandez, 1975; Levitt, 1990). The lifting anchorage systems are also designed based on concrete properties at a designated early age.

Proper control of early-age cracking risk in concrete as well as optimisation of relevant processes in precast industry therefore requires an adequate knowledge of tensile and fracture properties of the materials being considered. As a result, reliable data on complete tensile stress-strain curves of concrete at relevant ages are needed. Unfortunately, despite significant past research effort, such useful data are currently very limited, especially for concrete during the first hours after mixing. This is possibly mainly due to the considerable challenges in testing early-age concrete, which is both weak and wet. A number of direct tensile testing systems

have been developed, each with its own merits and drawbacks as detailed in (Nguyen & Dao, 2014, 2015). An improved testing system that can effectively address major drawbacks in available setups is therefore needed to enable the collection of more reliable data on early-age properties of concrete in direct tension.

In addition, it has also been suggested that aspects of early-age concrete performance can be improved through addition of fibres in concrete mixtures. Although being extensively studied and applied in practice since the late 1960s (Aly et al., 2008; Banthia & Gupta, 2006; Isabel & Ronald; Naaman et al., 2005; Qi et al., 2003; Rahmani et al., 2012; Ziad & Marc, 2002), such effects of fibres on performance of early-age concrete need further investigation to resolve remaining contradictions and unknowns. One of such remaining unknowns is the influence of different types of fibres on early-age tensile properties of concrete: There seems no reported literature on such influence despite its significance.

In this paper, an improved testing system that effectively overcomes major drawbacks in available test setups is first briefly described. Key aspects of the experimental study, relevant obtained test results and their discussion are then presented, followed by summary and conclusions.

DESCRIPTION OF THE DIRECT TENSILE TESTING SYSTEM AND TEST SERIES

The Direct Tensile Testing System

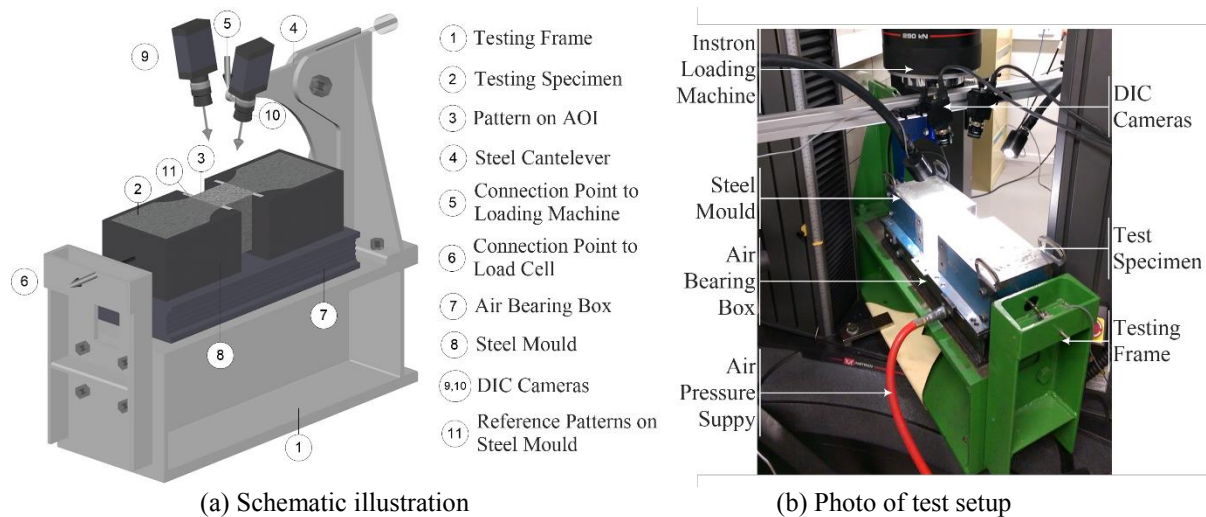


Figure 1 Direct tensile testing system.

Through critical evaluation of merits and drawbacks of available test systems, a new direct tensile testing system with significant improvements has been successfully developed at the University of Queensland. A schematic illustration of the new system, together with a photo of the actual setup, are shown in Figure 1. The test specimen is supported by an air-bearing box ⑦ and has one end fixed to the test frame ① through a load cell ⑥ and the other end being movable and connected to the loading machine ⑤. Notable features of this unique test apparatus include:

- The steel mould ⑧ is assembled using a magnetic table to ensure a planar bottom surface. The reduced middle region of test specimen has 100x70 mm² in cross-section and 70 mm in length (Figure 2).
- Air-bearing box ⑦: The upper plate of the air-bearing box has 32 holes symmetrically distributed under the two halves of the mould. The levelness of the upper surface of the air-bearing box after placement in the test position is ensured by using an electronic leveller with an accuracy of 0.1°. During testing, the air bearing box provides a uniform air pressure to float the test specimen, thereby effectively eliminating friction between the specimen and the supporting surface.
- Digital Image Correlation (DIC): The novel application of DIC enables the desired deformation over the whole Area of Interest (AOI, as shown in Figure 2) to be reliably captured in a non-contact way. The successful use of DIC in testing of concrete several hours after mixing has thus effectively addressed major shortcomings of previous set-ups. In this study, two high resolution professional DIC cameras (2448x2048 pixel) are employed to capture the 3D displacement/deformation of the top surface of concrete specimen. Both cameras (⑨,⑩ in Figure 1) are synchronized with the loading

process by a “sync” software developed in-house at The University of Queensland. Four reference pattern areas (11) (Figure 1) are also applied to the steel mould at four corners of the AOI to facilitate verification of displacement analysis from DIC system.

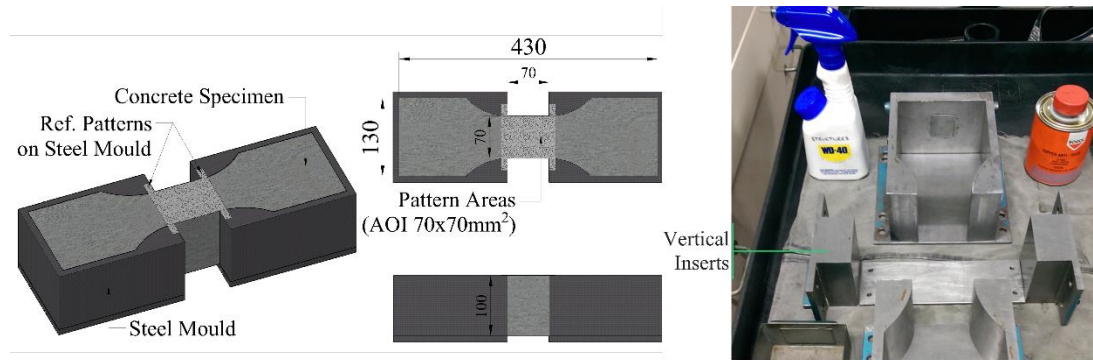


Figure 2 Testing mould and the Area of Interest.

Further details of the testing system, including the critical improvements compared to previous systems as well as the verifications to establish its effectiveness and reliability for early-age concrete testing, can be found elsewhere (Nguyen & Dao, 2014, 2015).

Concrete Mixes and Test Series

Table 1 Concrete mix design (30MPa – 80mm*)

Ingredients	Cement (kg)	20mm Hornfels (kg)	10mm Hornfels (kg)	Coarse Sand (kg)	Fine Sand (kg)	Water Reducer (L)	Water (L)	Micro Fibre** (kg)
Quantity/m ³	310	790	280	495	366	1.09	195	0.90

Notes: * 30MPa – characteristic compressive strength at 28 days and 80mm – slump;

** Micro fibre content is for micro fibre mix only; for normal mix, this amount is zero.

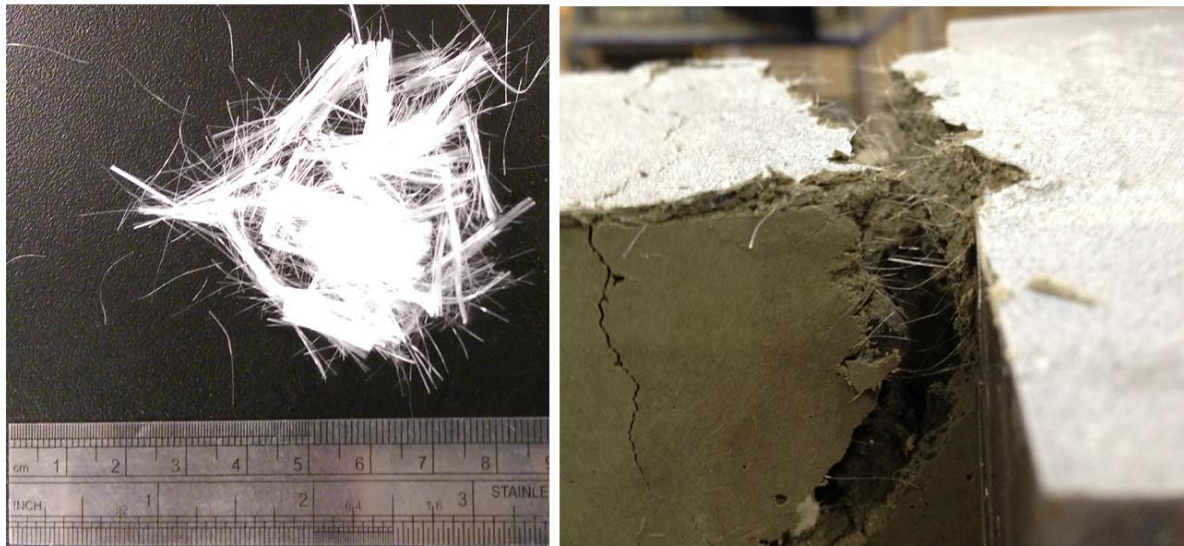
The selection of concrete type depends on its popularity in practice, as well as the susceptibility of the structural members (made of that concrete) to early-age cracking/damage. By that criteria, the concrete mixes 30MPa-80mm, with and without micro fibre were chosen (Table 1). For comparison, fibre content is the only difference between two mix designs. The chosen fibre is 12mm long micro filament made of 100% virgin blended-, non-fibrillating copolymer (Figure 3). Fibre’s specific gravity is 0.91 and its tensile strength ranges between 685 MPa and 758 MPa. The product follows ASTM C-1116, Type III, Section 4.1.3 “Synthetic Fiber-Reinforced Concrete and Shotcrete” (FIBERCON, 2015).

In order to have a comprehensive consideration over concrete properties, all ingredients were ensured to be consistent throughout the testing series and were maintained in the same laboratory conditions within the testing period. Regular moisture tests were conducted every three weeks for fine sand, coarse sand and 10mm Hornfels aggregate; from which the actual water amount could be adjusted accordingly. Oven was applied for the first moisture tests, while Speedy Moisture Meter was employed periodically afterward.

The mixing, placement and curing of concrete of both mixes were kept the same as far as practical to ensure similar mix quality. Assuming zero water absorption of the fibre as given in the product data sheets (FIBERCON, 2015), the effect of fibre on effective water content as well as water/cement ratio can be considered negligible.

Testing Procedures

Concrete was mixed by a medium rotating mixer of 70 litre capacity and placed directly into the steel mould, which was then compacted via a vibrating table. Test specimens were subsequently covered by three layers of dump cloth and transferred to the test room. The whole test series was conducted in an air-conditioned room with negligible wind, temperature (18-22°C) and humidity (55%-60%). Concrete age is measured from the time water is added to the mix.



(a) Micro fibres (b) Fibre distribution across a crack
 Figure 3 Micro fibres and their typical distribution across a crack surface.

The tensile testing frame was mounted onto the Instron loading machine (of 250 kN capacity) and kept in place by two steel clamps installed at two sides. One 2 kN load cell with high accuracy, the main load recording device, was installed at the fixed end of the testing frame. For each specimen, curing cloth layers were removed about 15 minutes before testing, leaving the top surface for pattern application, which is a vitally important step to ensure the quality of DIC analysis. Flat RustOleum industrial fast drying spray paint was chosen for pattern material due to its fast drying capacity as well as lowest gloss.

In order to put the mould into place, first of all an air pressure level of ~20psi (140kPa), which was sufficient to float the test specimen, was supplied. The test specimen was then carefully placed on the air table and its two ends were connected to the testing frame using rod end linkages and clevises. When the air was still on, an initial tensile load of approximately 0.1-0.2N was applied to ensure straight alignment and minimised initial “lag” at connections.

DIC camera system was then installed with the camera axes focusing on the centre of concrete’s top surface. Two cameras were employed into one 3D system. The angle formed by each camera axis and the vertical line perpendicular to the top surface was approximately 10°-20°, which is the optimal range for best analysis quality (www.correlatedsolutions.com, 2007). The distance from the camera lens to concrete surface was 20-25 cm. Each camera has a pixel resolution of 2448x2048, and intensity resolution of 8 bit. Camera capturing frequency was 2-5 seconds and the chosen displacement rate was 0.05mm/min.

RESULTS AND DISCUSSION

Throughout the whole test series, tensile stress data was determined from the readings of the 2 kN load cell, assuming uniform stress distribution on any given cross-section within AOI. Tensile strain was obtained from 3D analysis of VIC-3D program. The engineering strain ($\epsilon_{xx} = \Delta x/L$) was calculated manually from extracted displacement values over a fixed gauge length.

Figure 4 shows typical stress-strain curves obtained for different ages from mixing. The values of ultimate strain ϵ_o at full separation were also determined for the last tests of each series. From these obtained stress-strain curves, a number of important concrete properties at very early ages can be derived, including tensile strength, Young’s modulus, tensile strain capacity and fracture properties as discussed in the subsequent sections.

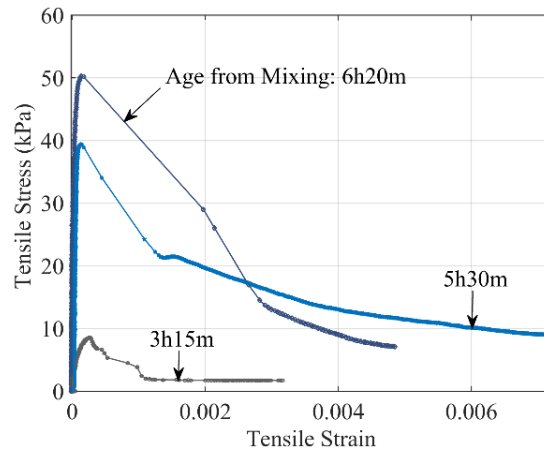


Figure 4 Typical obtained stress-strain relationships at different ages.

Tensile Strength f_t and Young's Modulus E_t development

The time evolution of tensile strength and Young's modulus is plotted in Figure 5. It can be observed that concrete tensile strength is negligibly small during the first 3 hours but accelerates quickly to several times larger in the next few hours (Figure 5a). A development trend is also observed, being in good agreement with previous studies although at different developing rates (V. T. N. Dao et al., 2009; Kasai et al., 1974). Such development is consistent with the hydration process: (i) The dormant period with minimal hydration lasts for approximately 2-4 hours for normal concrete as used in this study; (ii) Following initial set, significant ongoing hydration results in rapid increase in tensile strength (Department of Transportation (USA), 2007; Neville, 1986).

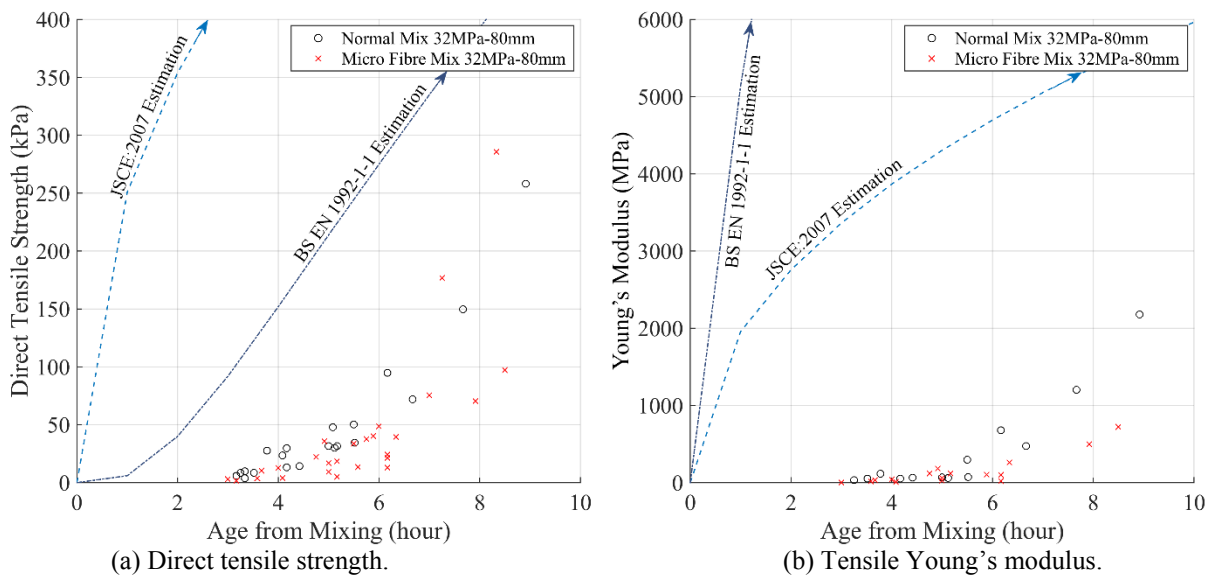


Figure 5 Development of tensile strength and Young's modulus.

Comparing the measured tensile strengths of less than 50 kPa during the first 6 hours after mixing as in Figure 5a with the possible maximum tensile stress in young concrete due to matric suction of higher than 60 kPa (V. T. N. Dao et al., 2008), the necessity of protecting early-age concrete is clear.

Further investigations regarding tensile strength of two test mixes gives the following characteristics:

- Recorded tensile strength of concrete without micro-fibre are more consistent therefore an obvious developing trend is formed. However, greater deviation in recorded results is observed for the case of micro-fibre mix, which commences from approximately 4 hours of age and further increases at later ages. Fibre distribution (including global- and local- fibre density), fibre alignment as well as the number of fibres present across a specific crack surface are thought to be contributory factors (RILEM

TC 162-TDF, 2001). Typical distribution of micro fibres across a concrete crack surface is shown in Figure 3.

- Visual inspection clearly indicates higher bleed water accumulated on the top surface of test specimens of micro-fibre mix, compared to those of mix without micro-fibre. This phenomenon is consistent with observations in other studies (Aly et al., 2008; Qi et al., 2003; Toutanji et al., 1998). Such increased bleeding is thought a result of fibres acting as tiny “fluid channels” along the length of fibres, facilitating vertical water movement.
- Interestingly, the direct tensile strength of micro-fibre mix in most cases is lower than that of normal mix without micro-fibre (Figure 5a). This is possibly due to the presence of micro-fibre in mix design: Since the fibres are chemically inert (FIBERCON, 2015), their bond with surrounding concrete mostly derives from the physical interaction and friction with the hydrated cement paste. Such bond might be smaller than the inherent bond within hydrated cement paste, thus compromising the tensile property of concrete specimens with micro-fibres. Moreover, concretes with fibre addition have been shown to have higher meso-pore sized porosity compared to that of the reference normal concrete (Aly et al., 2008).

The roles played micro-fibres in mitigating the risk of plastic shrinkage cracking are thus complex: (i) The possible decreased tensile strength heightens such risk; (ii) An increased bleeding discussed above helps reducing the risk; and (iii) The higher fracture energy and characteristic length, as discussed later, implies higher ductility.

It should also be noted that fibres and their positive effects on early defects such as plastic shrinkage cracking (from the first hour after mixing (Qi et al., 2003)) and drying shrinkage cracking (for hardened concrete) have been for decades investigated and acknowledged (Banthia & Gupta, 2006; Isabel & Ronald; Qi et al., 2003; Rahmani et al., 2012; Shah & Daniel, 1994; Ziad & Marc, 2002). Such studies have a similar approach which relies mainly on the strain-related criteria such as crack lengths, maximum crack widths as well as total crack areas. By such approach, the main focus is mostly placed on the ability of fibres in crack opening control, rather than cracking prevention. From Figure 5a, it clearly indicates a necessity to re-assess the role of fibre addition for young concrete in a more comprehensive way, incorporating pre-crack properties into consideration as well.

Young’s modulus has similar developing trend to that of tensile strength, although considerable increase is only observed from around 5 hours after mixing, as evidenced in Figure 5b. In this study, Young’s modulus is found by:

- Linear curve-fitting to the ascending part of stress-strain curves between ~5% and 40% of the tensile strength, following available standard (Standards Australia, 1997); in a combination with
- Visual inspection of the linear characteristic of the stress-strain curve within chosen range.

Once again, the obtained Young’s modulus for micro fibre mix is considerably lower than that for normal mix at most of testing ages (2.5-9 hours), both in value and rate/speed (Figure 5b).

Also in Figure 5, tensile strength and Young’s modulus development trend are also placed into a qualitative comparison with the estimation methods in currently available design standards. Eurocode’s BS EN 1992-1-1:2004 (British Standard, 2004) and Japanese’s JSCE: 2007 (JSCE Concrete Committee, 2007) are among very few (if not the only two) providing formulae to estimate early-age tensile properties. The estimation curves shown are determined for Ordinary Portland Cement and at the same designed characteristic compressive strength, with concrete ages input in day(s). In Figure 5a, BS EN 1992-1-1 seems to give a good agreement with this study over tensile strength’s development. For the case of Young’s modulus, both standards show differences both in value and in trend with this study and also differ significantly from each other.

Strain at Peak Stress ϵ_c

The time evolution of the obtained strain at peak stress is plotted in Figure 6, from which several characteristics can be identified, including:

- Strain at peak stress is observed to decrease over time for both mixes within the test age range (2.5-9 hours), and possibly reaching a minimum value at approximately 8-9 hours (Figure 6a). This corresponds well with minimum values at around 10 hours reported in (Kasai et al., 1972).

- Although with more variation, micro fibre mix experiences little difference between its strain at maximum stress and that of the reference normal mix in the first 5 hours after mixing (Figure 6a). However, for later ages (5-9 hours), a relatively higher level of strain at peak stress is observed, corresponding to that reported in (Ziad & Marc, 2002). Fibre-concrete bond development is thought to be the reason for such difference.
- A comparison with previous studies in Figure 6b indicates good agreement with this study in terms of basic trend and value. The lowest points appear at around 5-10 hours after mixing with the values ranging from $\sim 20\mu\epsilon$ (Roziere et al., 2015) to $\sim 150\mu\epsilon$ (Hannant et al., 1999; Kasai et al., 1972). It should be noted that concrete plastic shrinkage within 3-9 hours of age, depending on the amount of superplasticizer, is between $\sim 50\mu\epsilon$ and $1200\mu\epsilon$ (Holt & Leivo, 2004). With early-age concrete experiencing shrinkage that can be significantly higher than its strain capacity, the risk of early cracking and thus the critical need of an appropriate curing method are again clearly highlighted.

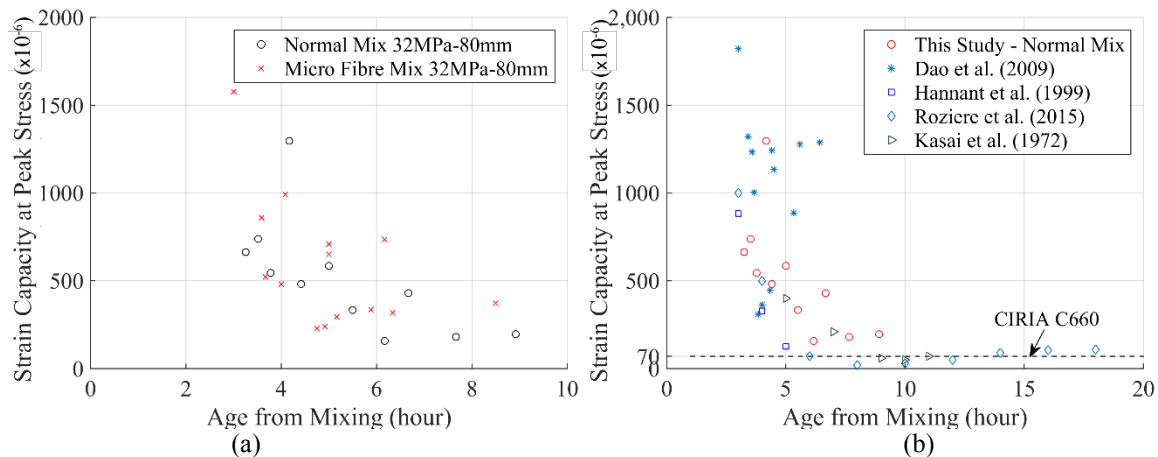


Figure 6 (a) Strain et peak stress evolution over time and (b) Comparison with previous studies, including (Bamforth, 2007; V. T. N. Dao et al., 2009; Hannant et al., 1999; Kasai et al., 1974; Roziere et al., 2015).

- Besides Eurocode's BS EN 1992-1-1:2004 (British Standard, 2004) and Japanese's JSCE: 2007 (JSCE Concrete Committee, 2007), CIRIA C660 (Bamforth, 2007) is among very few design specifications provided for early cracking control. The specification suggests tensile strain capacity as the design criteria, which is $70\mu\epsilon$ for all types of concrete (Figure 6b). Compared to this study as well as previous ones, such suggestion seems to be adequate for concrete without fibres but somewhat conservative for micro-fibre concrete.

Fracture Properties

Using the obtained test data, fracture properties can be calculated based on a stress-crack opening curve, following the fictitious crack model proposed by Hillerborg (Hillerborg, 1985). The development over time of fracture energy G_F , defined as the area under the stress-crack opening curve (excluding the elastic shortening when cracking occurs), is plotted in Figure 7a. From the figure:

- G_F is observed to increase over time, with more consistent trend for normal concrete without micro-fibre, compared to that of micro-fibre concrete. Fibre distribution and alignment as well as number of fibres crossing the fracture area are thought to be the main factors to cause greater variation of G_F in fibre mix (Löfgren et al., 2008). It should be noted that due to the very definition, fracture energy is very sensitive to the reliability of displacement measurement setup. A comparison with previous study (V. T. N. Dao et al., 2009) for the same mix design and similar testing system shows large difference in G_F 's development trend because of different displacement recording systems employed (Nguyen & Dao, 2015). This highlights the necessity of reliable measurement of displacement - The novel adoption of DIC system in this study for reliable non-contact displacement tracking method is therefore an important improvement.
- Within the testing period (2.5-9 hours), G_F of micro fibre mix is found to be slightly higher than that of the reference normal mix at a specific test age. As discussed previously, the addition of micro fibres

produces two counteracting effects on early-age concrete behaviour, which in turn deviate G_F . Lower tensile strength reduces G_F but at the same time, higher post-crack deformation increases it. Although the obtained results are generally in good agreement with other studies (Banthia & Gupta, 2006; Isabel & Ronald; Rahmani et al., 2012; Ziad & Marc, 2002), “high effectiveness” or “significant crack delay and reduction” of fibres are not observed in this study.

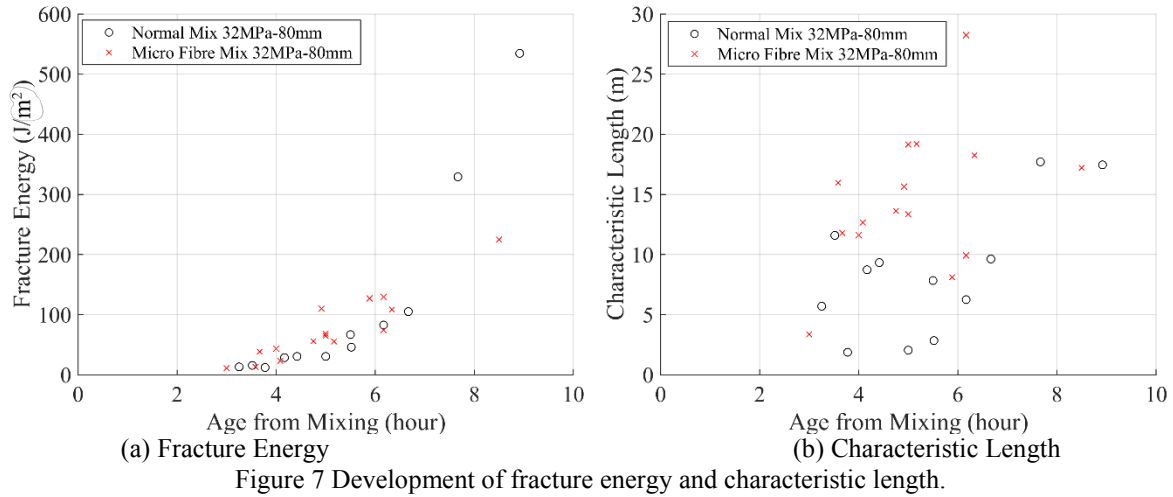


Figure 7b shows the characteristic length l_{ch} development:

- Although with large scatter due to the accumulation of different uncertainties in E_t , f_t and G_F , an increase trend from very low value (approximately 1-2m) is also observed for both mixes within 2.5-7 hours of age, which corresponds to Dao et al. (V. T. N. Dao et al., 2009) and Østergaard (Østergaard, 2003). From 7 hours after mixing, the trend seems to stabilize and slowly decrease at around 17m. If combined with the observation in previous study (Østergaard, 2003) for the ages after 10 hours, l_{ch} after reaching the indicated peak will decline, according to the growth of concrete brittleness.
- As the definition implies, l_{ch} is proportional to fracture energy G_F and to the inverse of tensile strength f_t . Therefore, with lower tensile strength f_t and higher value of G_F , the characteristic length of micro fibre mix clearly demonstrates higher values than that of the reference normal one, for most of test ages. Higher characteristic length of micro fibre mix indicates higher ductility, which is consistent with general understanding of basic roles of fibre addition (Karihaloo, 2015).

SUMMARY AND CONCLUSIONS

With the aim to address the knowledge gap of concrete tensile properties at very early ages, this study was conducted by employing an improved direct tensile testing system with the application of DIC displacement measurement method. Two mixes with and without synthetic micro fibre addition were investigated for their tensile properties of between 2.5 hours and 9 hours after mixing. The paper has presented key aspects of the employed testing system as well as discussion of obtained results. Major conclusions drawn in this paper include:

- Compared to concrete without micro-fibre, micro-fibre concrete has
 - more bleeding;
 - considerably lower and more scattered tensile strength and Young’s modulus;
 - similar values of strain at peak stress;
 - slightly higher fracture energy;
 - higher characteristic length.
- Possible explanations for such differences between concrete with and without micro-fibre are also given. The increased bleeding is likely a result of fibres acting as tiny “fluid channels” facilitating bleeding process. The possible lower bond between fibres and surrounding matrix compromises the tensile properties of concrete specimens with micro-fibres. Fibre distribution and alignment as well as the number and nature of fibres crossing crack surfaces contributes to the scatter of properties of micro-fibre concrete.

- The roles played by micro-fibres in mitigating the risk of plastic shrinkage cracking are thus complex, prompting the need for further study: Although a decreased tensile strength heightens such risk, an increased bleeding helps reduce the risk while the higher fracture energy and characteristic length implies higher ductility.

ACKNOWLEDGMENTS

The authors gratefully acknowledge the contribution of (i) following undergraduate students: Renee Shi, Denton Liu, Qiule Qu, Guanwei Zhang and Yang Xu; (ii) Technical staff within UQ School of Civil Engineering; and (iii) Fibercon.

REFERENCES

- Aly, T., Sanjayan, J. G., & Collins, F. (2008). Effect of polypropylene fibers on shrinkage and cracking of concretes. *Materials and Structures*, 41(10), 1741-1753.
- Bamforth, P. B. (2007). Early-Age Thermal Crack Control in Concrete *CIRIA C660*. London.
- Banthia, N., & Gupta, R. (2006). Influence of polypropylene fiber geometry on plastic shrinkage cracking in concrete. *Cement and Concrete Research*, 36(7), 1263-1267.
- British Standard. (2004). Eurocode 2: Design of concrete structures *Part 1-1: General rules and rules for buildings* (pp. 230). UK: British Standard.
- Byard, B., Schindler, A., Barnes, R., & Rao, A. (2010). Cracking tendency of bridge deck concrete. *Transportation Research Record: Journal of the Transportation Research Board*, 2164(-1), 122-131.
- Dao, V. N. T., Morris, P. H., & Dux, P. F. (2008). On equations for the total suction and its matric and osmotic components. *Cement and Concrete Research*, 38(11), 1302-1305.
- Dao, V. T. N., Dux, P. F., & Morris, P. H. (2009). Tensile properties of early-age concrete. *ACI Materials Journal*, 106(6), 483-492.
- Department of Transportation (USA). (2007). Integrated Materials and Construction Practices for Concrete Pavement: A State-of-the-Practice Manual. USA.
- FIBERCON. (2015). Fibercon Micro Poly Fibres for Concrete Reinforcing - Product Data. Accessed at www.fibercon.com.au on October 10 2015.
- Hannant, D. J., Branch, J., & Mulheron, M. (1999). Equipment for tensile testing of fresh concrete. *Magazine of Concrete Research*, 51, 263-267.
- Hernandez, H. D. (1975). *Time-dependent Prestress Losses in Pretensioned Concrete Construction*. PhD Thesis, University of Illinois at Urbana-Champaign, Ann Arbor.
- Hillerborg, A. (1985). The theoretical basis of a method to determine the fracture energy G_F of concrete. *Materials and Structures*, 18(4), 291-296.
- Holt, E., & Leivo, M. (2004). Cracking risks associated with early age shrinkage. *Cement and Concrete Composites*, 26(5), 521-530.
- Isabel, P., & Ronald, F. Z. Effect of synthetic fibers on volume stability and cracking of Portland cement concrete and mortar. *Materials Journal*, 87(4).
- JSCE Concrete Committee. (2007). English version of standard specification for Concrete Structures - 2007 *Design*. Japan: Japan Society of Civil Engineers.
- Karihaloo, B. L. (2015). A new approach to the design of RC structures based on concrete mix characteristic length. *International Journal of Fracture*, 191(1-2), 147-165.
- Kasai, Y., Yokoyama, K., & Matsui, I. (1972). Mechanical Behavior of Materials. *Society of Materials Science*, 4.
- Kasai, Y., Yokoyama, K., Matsui, I., & Tobinai, K. (1974). Tensile properties of early-age concrete. 433-441.
- Levitt, M. (1990). Production - Specific Processes *Precast Concrete*: Spon Press.
- Löfgren, I., Stang, H., & Olesen, J. F. (2008). The WST method, a fracture mechanics test method for FRC. *Materials and Structures*, 41(1), 197-211.
- Naaman, A. E., Wongtanakitcharoen, T., & Hauser, G. (2005). Influence of different fibers on plastic shrinkage cracking of concrete. *ACI Materials Journal*, 102(1), 49-58.
- Neville, A. M. (1986). *Properties of concrete*. London: Longman Scientific & Technical.
- Nguyen, D., & Dao, V. (2014). *A novel method for tensile testing of very early-age concrete*. Proceedings of the 23rd Australasian Conference on the Mechanics of Structures and Materials (ACMSM23), Byron Bay, Australia: 47-52.
- Nguyen, D., & Dao, V. (2015). *Tensile properties of early-age concrete*. Proceedings of the 27th Biennial National Conference of the Concrete Institute of Australia in conjunction with the 69th RILEM Week, Melbourne, Australia: 1314-1324.
- Østergaard, L. (2003). *Early Age Fracture Mechanics and Cracking of Concrete*.

- Qi, C., Weiss, J., & Olek, J. (2003). Characterization of plastic shrinkage cracking in fiber reinforced concrete using image analysis and a modified Weibull function. *Materials and Structures*, 36(6), 386-395.
- Rahmani, T., Kiani, B., Bakhshi, M., & Shekarchizadeh, M. (2012). *Application of different fibers to reduce plastic shrinkage cracking of concrete*.
- RILEM TC 162-TDF. (2001). Test and design methods for steel fibre reinforced concrete - Uni-axial tension test for steel fibre reinforced concrete. *Materials and Structures*, 34, 3-6.
- Roziere, E., Cortas, R., & Loukili, A. (2015). Tensile behaviour of early age concrete: New methods of investigation. *Cement and Concrete Composites*, 55(0), 153-161.
- Shah, S. P., & Daniel, J. I. (1994). *Fiber reinforced concrete: developments and innovations* (SP-142). American Concrete Institute.
- Springenschmid, R. (1994). *Thermal cracking in concrete at early ages* (R. Springenschmid Ed.). London: E & FN Spon.
- Springenschmid, R. (1998). *Prevention of thermal cracking in concrete at early ages*.
- Standards Australia. (1997). Methods of testing concrete - AS1012.17 *Method 17: Determination of the static chord modulus of elasticity and Poisson's ratio of concrete specimens*. Australia.
- Toutanji, H., McNeil, S., & Bayasi, Z. (1998). Chloride permeability and impact resistance of polypropylene-fiber-reinforced silica fume concrete. *Cement and Concrete Research*, 28(7), 961-968.
- Wiss, J., Elstner Associates, Inc. (2011). On-call structural concrete bridge deck cracking investigation services *WJE No. 2009.2643*. Emeryville, California 94608: Wiss, Janney, Elstner Associates, Inc.
- www.correlatedsolutions.com. (2007). *Vic-3D 2007 Testing Guide* (57 p.).
- Ziad, B., & Marc, M. (2002). Application of fibrillated polypropylene fibers for restraint of plastic shrinkage cracking in silica fume concrete. *Materials Journal*, 99(4).